



Imaging diagnosis of lumbar foraminal stenosis in the fifth lumbar nerve root: reliability and reproducibility of T1-weighted three-dimensional lumbar MRI

Ko Hashimoto^{1,2}, Yasuhisa Tanaka², Takumi Tsubakino², Takeshi Hoshikawa³, Tomowaki Nakagawa³, Takashi Inawashiro⁴, Kohei Takahashi^{1,2}, Masaru Suda⁵, Toshimi Aizawa¹

¹Department of Orthopaedic Surgery, Tohoku University Graduate School of Medicine, Sendai, Japan; ²Department of Orthopaedic Surgery, Tohoku Central Hospital, Yamagata, Japan; ³Department of Orthopaedic Surgery, Sendai Orthopaedic Hospital, Sendai, Japan; ⁴Department of Orthopaedic Surgery, Sendai City Hospital, Sendai, Japan; ⁵Department of Radiology, Tohoku Central Hospital, Yamagata, Japan

Contributions: (I) Conception and design: K Hashimoto, Y Tanaka; (II) Administrative support: Y Tanaka, T Aizawa; (III) Provision of study materials and patients: K Hashimoto, Y Tanaka, T Tsubakino, T Hoshikawa, T Nakagawa, T Inawashiro; (IV) Collection and assembly of data: K Hashimoto, Y Tanaka, T Tsubakino, T Hoshikawa, T Nakagawa, T Inawashiro, K Takahashi; (V) Data analysis and interpretation: K Hashimoto, K Takahashi, T Aizawa; (VI) Manuscript writing: All authors; (VII) Final approval of manuscript: All authors.

Correspondence to: Ko Hashimoto, MD, PhD. Department of Orthopaedic Surgery, Tohoku Central Hospital, 3-2-5 Wago-machi, Yamagata, Yamagata 990-8510, Japan. Email: khashimoto@med.tohoku.ac.jp.

Background: Various magnetic resonance imaging (MRI) techniques have been reported in detection of lumbar foraminal stenosis (LFS), especially for T2-weighted three-dimensional MRI (3D-MRI) describing the shape of nerve roots. The detection of LFS in the fifth lumbar nerve root (L5 root), however, is still less reliable compared to other lumbar nerve roots. Then we have been using T1-weighted 3D-MRI aiming to depict the shape of, and also pathology affecting the L5 root. The aim of this study is to evaluate our T1-weighted 3D-MRI in diagnosing LFS of the L5 root.

Methods: This retrospective study included 24 patients with intracanal stenosis (ICS) at L4-5, and 30 patients with LFS at L5-S causing unilateral L5 root lesion. The pre-operative T1-weighted 3D-MRI aiming bilateral L5 nerve roots of each patient were blinded and reviewed twice by five spine surgeons, independently. The image evaluation was performed in two conditions: (I) the symptomatic side was judged in 30 patients of LFS patients, and (II) the symptomatic side or the absence of LFS was judged in images of all the 54 patients including LFS and ICS patients. The correct-answer-rate, sensitivity and specificity of the imaging study were calculated. Also, the intra- and interobserver agreement of the imaging study by five spine surgeons were evaluated by the kappa (κ) statistics.

Results: For conditions (I) and (II) above, the mean correct-answer-rate was 92.3% and 69.8%, respectively. The sensitivity and specificity of the imaging study was 72.6% and 66.3%, respectively. The average of intraobserver κ -value of five examiners was 0.874 and 0.708, and the average of interobserver κ -value was 0.837 and 0.578, respectively.

Conclusions: As well as previously reported T2-weighted 3D-MRI, our T1-weighted 3D-MRI was found to be reliable in diagnosing LFS of the L5 root.

Keywords: Lumbar foraminal stenosis (LFS); fifth lumbar nerve root (L5 root); three-dimensional magnetic resonance imaging (3D-MRI); T1-weighted images; reliability; reproducibility; intraobserver agreement; interobserver agreement

Submitted Jul 08, 2021. Accepted for publication Aug 26, 2021.

doi: 10.21037/jss-21-63

View this article at: <https://dx.doi.org/10.21037/jss-21-63>

Introduction

Imaging diagnosis of lumbar foraminal stenosis (LFS) has been challenging as conventional imaging techniques could not describe the pathology at the foraminal part clearly (1). In these years, various magnetic resonance imaging (MRI) techniques have been reported in detection of LFS thanks to recent technical progress (2-12). To date, T2-weighted three-dimensional MRI (3D-MRI) has been dominantly employed and reported in diagnosis of LFS by describing the shape of nerve roots (2-4,12). Even with those advanced imaging techniques, detection of LFS in the fifth lumbar nerve root (L5 root) is still less reliable compared to other lumbar nerve roots (2,12), presumably because of complexed anatomy of the L5 root tract including variant shape of the L5 transverse process, the presence of sacral ala and so on. Then, we have been using T1-weighted 3D-MRI since T1-weighted images can depict not only the shape of nerve root from intracanal to extraforaminal area, but also perineural soft tissues such as ligamentum flavum and intervertebral disc material (5,6). Although each report advocates the benefit of 3D-MRI in diagnosing LFS (2-4,7,9,11), few reports have validated the reliability or reproducibility only by T2-weighted 3D-MRI (11,12), not by T1-weighted 3D-MRI. The aim of this study is to evaluate our T1-weighted 3D-MRI in diagnosing LFS of the L5 root by assessing its correct-answer-rate, sensitivity, specificity, and intra- and interobserver reproducibility.

We present the following article in accordance with the STARD reporting checklist (available at <https://dx.doi.org/10.21037/jss-21-63>).

Methods

Patients

The study was conducted in accordance with the Declaration of Helsinki (as revised in 2013). The study was approved by institutional ethics board of Tohoku University Graduate School of Medicine (Approval Number: 2014-1-495) and individual consent for this retrospective analysis was waived. This retrospective study included a total of 54 patients with unilateral L5 root lesion; 24 patients with intracanal stenosis (ICS) at L4-5 successfully treated only by ipsilateral partial laminotomy at L4-5 (i.e., no LFS: control), and 30 patients with LFS at L5-S successfully treated only by lateral fenestration at L5-S. The partial laminotomy includes fenestration of L4 lamina and inner edge of L5 superior articular process, ensuring decompression of

intracanal part of the branching L5 nerve root by the inner edge of L5 pedicle. The lateral fenestration includes partial resection of the lateral part of L5 pars interarticularis, the caudal part of L5 transverse process and the cranial part of sacral ala, enabling extraforaminal decompression of L5 nerve root. The demographic data of the objectives are shown in *Table 1*.

Coronal and oblique-coronal T1-weighted MRI

3D-MRI was performed with MAGNETOM Avanto™, a 1.5-T scanner using a spinal coil (SIEMENS, Munich, Germany). The 3D-fast low angle shot (3D-FLASH), a gradient echo (GRE) scan technique, was used to obtain T1-weighted 3D images. The precise imaging conditions are shown in *Table 2*. In order to obtain coronal and oblique-coronal images showing a whole-length image of bilateral L5 nerve roots from their bifurcation from the dural sac to the extraforaminal part in one section, the multi-planar reconstruction (MPR) method was employed on a workstation (*Figure 1*). The precise methods for generating coronal image showing the L5 root in a slice from the branching point from the thecal sac to extraforaminal area, are shown in *Figure 2*. All images were acquired preoperatively.

Imaging analysis

The L5 roots were judged to have foraminal stenosis or compression by examiners when the images demonstrated swelling or horizontalization of the root at foraminal zone due to osteophytes or pushing-up sacral superior articular process, foraminal or extraforaminal disc herniation and so on, as indicated in the previous studies (2,12,13) (*Figure 3*). The images were evaluated in two conditions: (I) situations in general practice is simulated by giving preliminary information about the presence of LFS to examiners, and (II) the mixture of image data from LFS and ICS (no LFS: control) patients are evaluated without any preliminary clinical information. For condition (I), the symptomatic side was judged in 30 patients of LFS with given information about the presence of LFS in either side, and for condition (II), the symptomatic side or the absence of LFS was judged in images of all the 54 patients; a random mixture of LFS and ICS (no LFS: control), without given information about the presence or absence of LFS. For each condition, the image sets were evaluated twice in 2- to 4-week interval by five spine surgeons (board-certified orthopaedic surgeons

Table 1 Demographic data of the patients

Type of stenosis	L4-5 ICS	L5-S LFS
Number of patients (male: female)	24 (11:13)	30 (16:14)
Patients' age (years; mean \pm SD)	46–86 (65.5 \pm 9.3)	32–84 (59.6 \pm 14.2)

ICS, intracanal stenosis; LFS, lumbar foraminal stenosis; SD, standard deviation.

Table 2 Scanner settings for 3D-FLASH MRI

Setting element	Parameter
Orientation	Coronal
Phase encoding direction	R>L
Phase oversampling	90%
Slice oversampling	29%
Slice per slab	56
Flip angle	30°
Base resolution	256
Phase resolution	100%
Dimension	3D
PAT mode	GRAPPA \times 2
FOV	260 \times 191 mm
Voxel size	1 \times 1 \times 1.2 mm
Slice thickness	1.2 mm
TR	30 ms
TE	4.76 ms
Fat suppression	Non
Slice resolution	75%
RF spoiling	On
Band width	130 Hz/Px
RF pulse type	Normal
Gradient mode	Normal
Scan time	5 min 0 sec

3D-FLASH, three-dimensional fast low angle shot; MRI, magnetic resonance imaging; PAT, parallel acquisition technique; FOV, field-of-view; TR, repetition time; TE, echo time; RF, radiofrequency.

with >20-year experience with >5-year experience in spine surgery), independently, by shuffling the order of the image sets.

Statistical analysis

The reliability was evaluated by the rate of correct answer of each examiner and trial, and sensitivity and specificity calculated by combining the results of two reviews by five examiners (ten reviews altogether). Also, the intra- and interobserver agreement of the imaging study were evaluated by the kappa (κ) statistics (14). The κ -value is a serial statistical variable, indicating the extent of agreement between two data sets. The agreement is graded by the κ -value as shown in *Table 3* (14). The intraobserver κ -value was calculated by two reviews of each examiner. Also, the interobserver agreement of ten reviews (five examiners \times two reviews) was calculated in a round-robin manner (40 combinations in total). The mean κ -value was also calculated for intra- and interobserver agreement.

Results

The correct-answer-rate of the imaging studies of (I) the 30 patients of LFS and (II) all the 54 patients of ICS and LFS by ten reviews (five examiners \times two reviews) ranged from 86.7% to 96.7% (average: 92.3%), and 64.8% to 74.1% (average: 69.8%), respectively. The detailed data is shown in *Table 4*. The sensitivity and specificity of the ten reviews ranged from 60.0% to 80.0% (average: 72.6%) and 58.3% to 79.1% (average: 66.7%), respectively. The detailed data is shown in *Table 5*. The intraobserver κ -values of the ten reviews calculated in the condition (I) and (II) ranged from 0.714 to 1.000 (average: 0.874; “almost perfect”

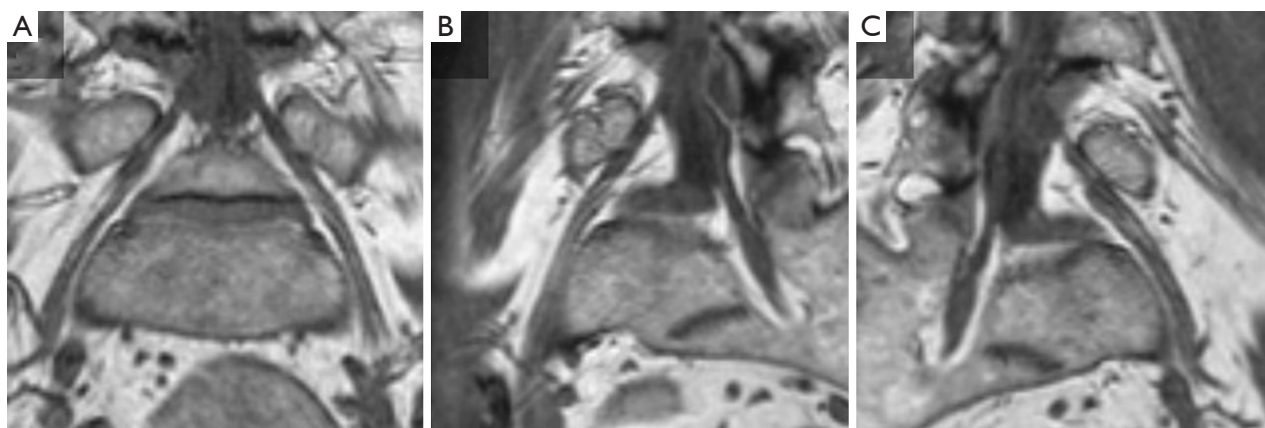


Figure 1 T1-weighted 3D-MRI used for the study. (A) Coronal section; (B) right oblique-coronal section; (C) left oblique-coronal section. 3D-MRI, three-dimensional magnetic resonance images.

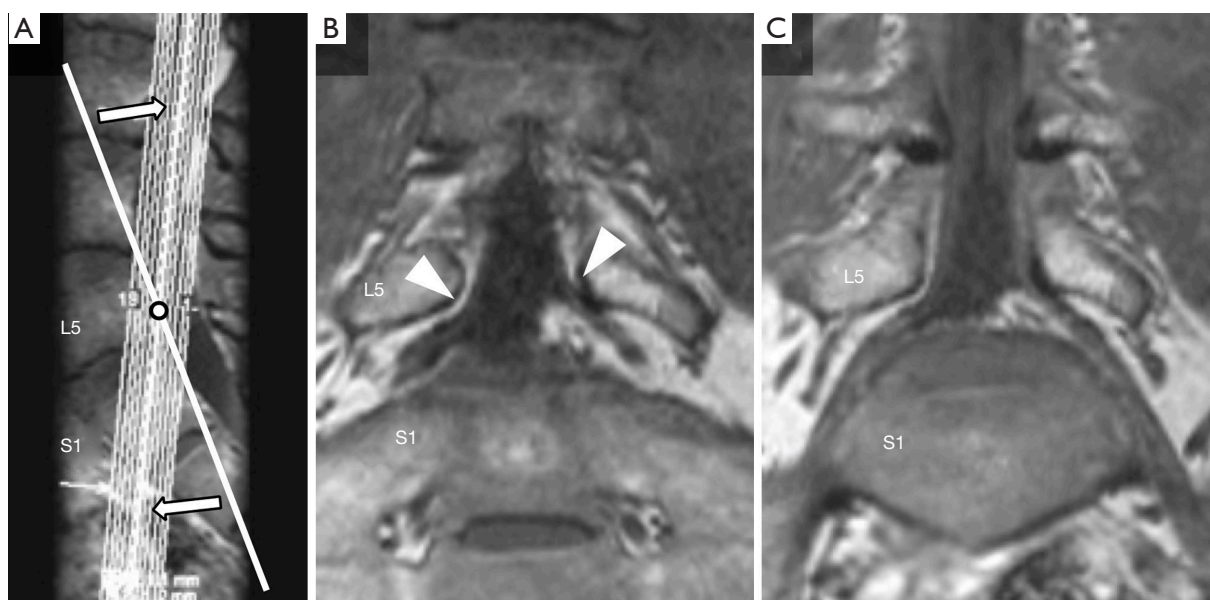


Figure 2 Generating methods of the coronal L5 root image by MPR. On a sagittal scout view, a reference point [open black circle in (A)] is set to depict the branching point of the L5 root from the thecal sac in the coronal view [arrow heads in (B)]. Then the image plane [white line in (A)] is rotated backward for 20 to 40 degrees from the posterior border of the L5 vertebral body using the reference point as rotation center (open black arrows), until the L5 root is shown in a slice from branching part to extraforaminal zone in the coronal view (C). L5, fifth lumbar; MPR, multi-planar reconstruction.

agreement) and 0.564 to 0.769 (average: 0.708; “substantial” agreement), respectively. The interobserver κ -values calculated in a round-robin manner (40 combinations in total) ranged from 0.727 to 0.933 (average: 0.850; “almost perfect” agreement) and 0.428 to 0.764 (average: 0.578; “moderate” agreement), respectively. The precise data of the intra- and interobserver agreement is demonstrated in

Figure 4.

Discussion

Standard two-dimensional MRI (2D-MRI) sequences are commonly used to detect nerve compression in degenerative lumbar spinal diseases; however, they sometimes

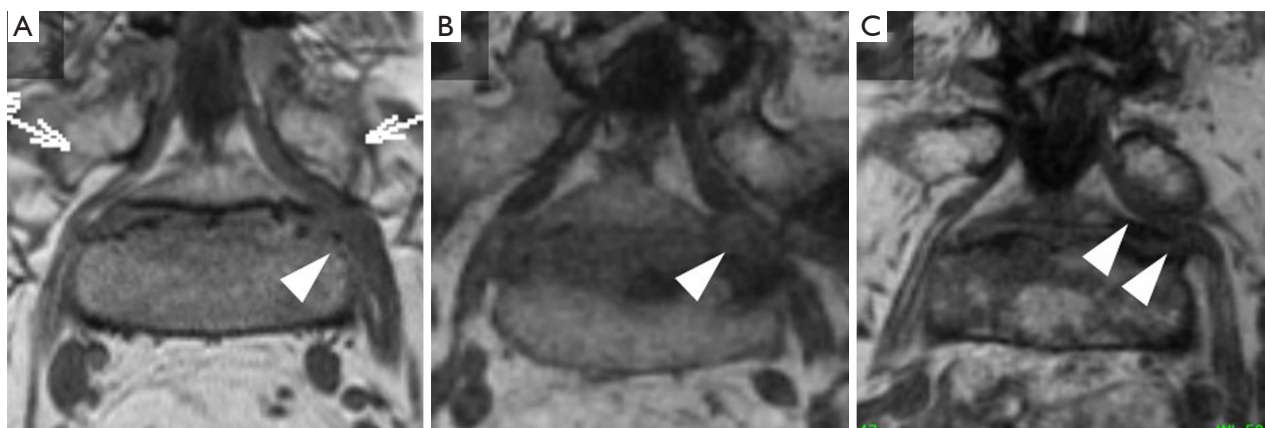


Figure 3 Examples of the findings of foraminal stenosis of the L5 nerve root. (A) Nerve root swelling (arrow head); (B) disc herniation (arrow head); (C) horizontalization of the nerve root (arrow heads). L5, fifth lumbar.

Table 3 Evaluation of intra- and inter-observer agreement by κ -value (14)

κ -value	Evaluation
<0	Poor
0–0.20	Slight
0.21–0.40	Fair
0.41–0.60	Moderate
0.61–0.80	Substantial
0.81–1.00	Almost perfect

Table 4 Correct-answer-rate of T1-weighted 3D-MRI in diagnosing L5-S foraminal stenosis for individual observers

Examiner	Correct-answer-rate of the reads of 30 LFS patients (%), (1 st /2 nd read)	Correct-answer-rate of the reads of all 54 ICS & LFS patients (%), (1 st /2 nd read)
A	96.7/96.7	66.7/68.5
B	93.3/86.7	72.2/64.8
C	90.0/90.0	70.4/74.1
D	93.3/96.7	74.1/74.1
E	93.3/86.7	66.7/66.7
Average	93.3/91.3	70.0/69.6
Overall, average \pm SD	92.3 \pm 3.9	69.8 \pm 3.6

3D-MRI, three-dimensional magnetic resonance imaging; LFS, lumbar foraminal stenosis; ICS, intracanal stenosis; SD, standard deviation.

Table 5 Sensitivity and specificity of T1-weighted 3D-MRI in diagnosing L5-S foraminal stenosis for individual observers

Examiner	Sensitivity (%), (1 st /2 nd review)	Specificity (%), (1 st /2 nd review)
A	73.3/80.0	58.3/54.2
B	73.3/63.3	70.8/66.7
C	76.7/83.3	62.5/62.5
D	80.0/70.0	66.7/79.1
E	60.0/66.7	75.0/66.7
Mean	72.7/72.7	66.7/65.8
Overall, mean \pm SD	72.7 \pm 7.7	66.3 \pm 7.5

3D-MRI, three-dimensional magnetic resonance imaging; SD, standard deviation.

cannot depict the nerve compression of LFS (15-19). In such situations, 3D-MRI is utilized as additional examination. To date, T2-weighted 3D-MRI has been dominantly reported (2,12), however, we have been using T1-weighted 3D-MRI for the purpose in an assumption that nerve-compressing factors such as osteophytes and disc herniation could be clearly delineated as well as nerve roots themselves (5,6). Also, our T1-weighted GRE method has a benefit of shortened scan time (5 minutes). Patients with LFS sometimes suffer from severe sciatica and experience intolerable pain during a long MRI scan time, resulting in motion artifact (20). T1-weighted GRE 3D-MRI can be beneficial especially for patients with severe leg pain

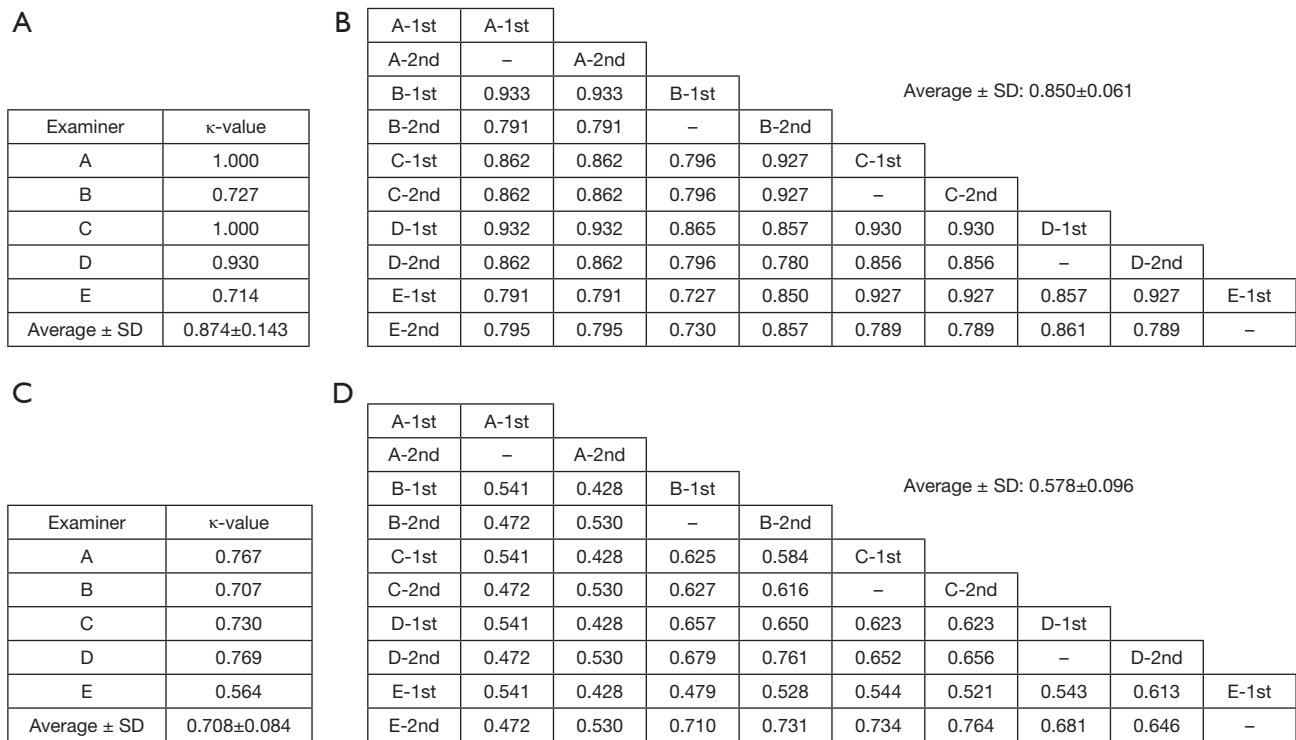


Figure 4 Intra- and interobserver agreement (κ-value) of the two readings by five spine surgeons. (A,B) Intra-, and interobserver agreement of judgements in 30 patients of LFS with given information about the presence of LFS, respectively. (C,D) Intra-, and interobserver agreement of judgements in 54 patients (ICS and LFS are combined) without given information about the absence or presence of LFS, respectively. Interobserver agreement was calculated in a round-robin manner of two reviews by five examiners (40 combinations in total). The first review of examiner A is shown as “A-1st”, for example. LFS, lumbar foraminal stenosis; ICS, intracanal stenosis; SD, standard deviation.

compared to T2-weighted 3D-MRI which takes longer scan time. Meanwhile, the correct-answer-rate and reliability of those imaging diagnosis have been still demonstrated mainly in T2-weighted 3D-MRI (2,12) although recent report demonstrated a study evaluating reliability in diagnosing LFS using T1-weighted high-resolution 2D-MRI (21).

In diagnosis of LFS, symptomatology and neurological diagnosis are obviously essential. Meanwhile, the correct-answer-rate and reliability of imaging diagnosis were assumed to be affected by the absence and presence of the information about neurological diagnosis. For this reason, we evaluated and compared the correct-answer-rate and reliability of the imaging diagnosis among the situation with and without given pre-information about the presence of LFS to the examiners. In this manner, the condition with given pre-information can simulate the situation in general practice where clinical information is already given to examiners before evaluating images, and the condition

without given pre-information can evaluate the diagnostic reliability of the imaging study itself. In our study, the correct-answer-rate and reliability were very high with given information about the existence of LFS, but were low when the images were randomly shown in the mixture without and with LFS, as expected. These results indicated that the prior recognition of LFS through neurological diagnosis is important to improve the correct-answer-rate and reliability of the imaging studies in patients with LFS.

The sensitivity in diagnosis of LFS in our study were 77%, which was lower than the previous reports by Aota *et al.* (2) (96%), evaluated in T2-weighted 3D-MRI. Aota *et al.* (2) evaluated all the foramens through L2-3 to L5-S in 90 LFS patients and 27 healthy volunteers in random order. Among 234 L5-S foramens reviewed, only 15 symptomatic foraminal stenosis was included. The positive predictive value of 7% and false positive rate of 48% in diagnosis of symptomatic L5-S foraminal stenosis indicated that the

reliability of their imaging diagnosis may not be necessarily high for L5-S foraminal stenosis. On the other hand, the specificity of 66% in our study was lower than the report by Yamada *et al.* (12) (98.3%). The authors focused on L5-S segment and validated the images of 60 LFS patients and 20 healthy volunteers. In their study, the mean age of L5-S foraminal stenosis group and healthy control group was 70.0 and 21.3 years, respectively. The specificity, in other words, the true negative rate is expected to be high when the population of control group is younger with less spondylotic changes in their lumbar spine. Our study focused on L5-S segment for foraminal stenosis, and set age-matched patients with unilateral L5 radiculopathy due to L4-5 ICS as a control group. For these points of view, we believe that our study provided practical validation of our T1-based 3D-MRI although the sensitivity and specificity were lower than the previous studies based on T2-weighted images. However, in order to compare the diagnostic values of T1- and T2-weighted images directly, further prospective studies are required using the images obtained from identical patients.

The intra- and interobserver agreement were precisely investigated by Yamada *et al.* (12) using their T2-based 3D-MRI. In their study, three examiners independently assessed the images twice in 1-month interval without given information about absence or presence of LFS. The mean intra- and interobserver κ -value were 0.8968 and 0.7933, respectively. On the other hand, our study was conducted by five examiners, and demonstrated the mean intra- and interobserver κ -value of 0.847 and 0.708, respectively. Compared to the previous study, the present study demonstrated equivalently high agreement on both intra- and interobserver reproducibility with more examiners than the previous studies. The reason for higher interobserver agreement could attribute to the expertise of the experienced examiners in evaluation of T1-weighted 3D-MRI, clearly detected L5 nerve root by T1-weighted images, or the condition of the study in which spinal level of the assessment was limited to L5-S.

There are some limitations to be considered in the present study. The number of the assessed patients and images were relatively small to generalize the results. Moreover, the exact superiority of T1- or T2-weighted images cannot be directly evaluated since images were not compared for the same patients in identical conditions, and ROC analysis was not performed to confirm the diagnostic accuracy in the present study. The stenotic factors such as nerve root swelling were not included in the analysis

which would give more precise information to the study. Also, spatial resolution of the images could not be elevated like high-resolution MRI because of the limitation in the specification of the MRI device and time available for each scan.

In conclusion, our T1-weighted 3D-MRI was found to be considerably reliable in diagnosing LFS of the L5 root same as the previous studies using T2-weighted 3D-MRI. Further studies are expected to elucidate and compare benefits and drawbacks of T1- or T2-weighted 3D-MRI.

Acknowledgments

Funding: None.

Footnote

Reporting Checklist: The authors have completed the STARD reporting checklist. Available at <https://dx.doi.org/10.21037/jss-21-63>

Data Sharing Statement: Available at <https://dx.doi.org/10.21037/jss-21-63>

Conflicts of Interest: All authors have completed the ICMJE uniform disclosure form (available at <https://dx.doi.org/10.21037/jss-21-63>). The authors have no conflicts of interest to declare.

Ethical Statement: The authors are accountable for all aspects of the work in ensuring that questions related to the accuracy or integrity of any part of the work are appropriately investigated and resolved. The study was conducted in accordance with the Declaration of Helsinki (as revised in 2013). The study was approved by institutional ethics board of Tohoku University Graduate School of Medicine (Approval Number: 2014-1-495) and individual consent for this retrospective analysis was waived.

Open Access Statement: This is an Open Access article distributed in accordance with the Creative Commons Attribution-NonCommercial-NoDerivs 4.0 International License (CC BY-NC-ND 4.0), which permits the non-commercial replication and distribution of the article with the strict proviso that no changes or edits are made and the original work is properly cited (including links to both the formal publication through the relevant DOI and the license). See: <https://creativecommons.org/licenses/by-nc-nd/4.0/>.

References

1. Macnab I. Negative disc exploration. An analysis of the causes of nerve-root involvement in sixty-eight patients. *J Bone Joint Surg Am* 1971;53:891-903.
2. Aota Y, Niwa T, Yoshikawa K, et al. Magnetic resonance imaging and magnetic resonance myelography in the presurgical diagnosis of lumbar foraminal stenosis. *Spine (Phila Pa 1976)* 2007;32:896-903.
3. Byun WM, Jang HW, Kim SW. Three-dimensional magnetic resonance rendering imaging of lumbosacral radiculography in the diagnosis of symptomatic extraforaminal disc herniation with or without foraminal extension. *Spine (Phila Pa 1976)* 2012;37:840-4.
4. Byun WM, Kim JW, Lee JK. Differentiation between symptomatic and asymptomatic extraforaminal stenosis in lumbosacral transitional vertebra: role of three-dimensional magnetic resonance lumbosacral radiculography. *Korean J Radiol* 2012;13:403-11.
5. Hasegawa T, An HS, Haughton VM. Imaging anatomy of the lateral lumbar spinal canal. *Semin Ultrasound CT MR* 1993;14:404-13.
6. Hasegawa T, Mikawa Y, Watanabe R, et al. Morphometric analysis of the lumbosacral nerve roots and dorsal root ganglia by magnetic resonance imaging. *Spine (Phila Pa 1976)* 1996;21:1005-9.
7. Heo DH, Lee MS, Sheen SH, et al. Simple oblique lumbar magnetic resonance imaging technique and its diagnostic value for extraforaminal disc herniation. *Spine (Phila Pa 1976)* 2009;34:2419-23.
8. Kikkawa I, Sugimoto H, Saita K, et al. The role of Gd-enhanced three-dimensional MRI fast low-angle shot (FLASH) in the evaluation of symptomatic lumbosacral nerve roots. *J Orthop Sci* 2001;6:101-9.
9. Lee IS, Kim HJ, Lee JS, et al. Extraforaminal with or without foraminal disk herniation: reliable MRI findings. *AJR Am J Roentgenol* 2009;192:1392-6.
10. Lee S, Lee JW, Yeom JS, et al. A practical MRI grading system for lumbar foraminal stenosis. *AJR Am J Roentgenol* 2010;194:1095-8.
11. Moon KP, Suh KT, Lee JS. Reliability of MRI findings for symptomatic extraforaminal disc herniation in lumbar spine. *Asian Spine J* 2009;3:16-20.
12. Yamada H, Terada M, Iwasaki H, et al. Improved accuracy of diagnosis of lumbar intra and/or extra-foraminal stenosis by use of three-dimensional MR imaging: comparison with conventional MR imaging. *J Orthop Sci* 2015;20:287-94.
13. Hasegawa T, An HS, Haughton VM, et al. Lumbar foraminal stenosis: critical heights of the intervertebral discs and foramina. A cryomicrotome study in cadavera. *J Bone Joint Surg Am* 1995;77:32-8.
14. Landis JR, Koch GG. The measurement of observer agreement for categorical data. *Biometrics* 1977;33:159-74.
15. Green RA, Saifuddin A. Whole spine MRI in the assessment of acute vertebral body trauma. *Skeletal Radiol* 2004;33:129-35.
16. Mascalchi M, Dal Pozzo G, Bartolozzi C. Effectiveness of the Short TI Inversion Recovery (STIR) sequence in MR imaging of intramedullary spinal lesions. *Magn Reson Imaging* 1993;11:17-25.
17. Modic MT, Ross JS. Lumbar degenerative disk disease. *Radiology* 2007;245:43-61.
18. Sirvanci M, Kara B, Duran C, et al. Value of perineural edema/inflammation detected by fat saturation sequences in lumbar magnetic resonance imaging of patients with unilateral sciatica. *Acta Radiol* 2009;50:205-11.
19. Tanitame K, Tanitame N, Tani C, et al. Evaluation of lumbar nerve root compression using thin-slice thickness coronal magnetic resonance imaging: three-dimensional fat-suppressed multi-shot balanced non-steady-state free precession versus three-dimensional T1-weighted spoiled gradient-recalled echo. *Jpn J Radiol* 2011;29:623-9.
20. Baskaran V, Pereles FS, Russell EJ, et al. Myelographic MR imaging of the cervical spine with a 3D true fast imaging with steady-state precession technique: initial experience. *Radiology* 2003;227:585-92.
21. Sartoretto E, Wyss M, Alfieri A, et al. Introduction and reproducibility of an updated practical grading system for lumbar foraminal stenosis based on high-resolution MR imaging. *Sci Rep* 2021;11:12000.

Cite this article as: Hashimoto K, Tanaka Y, Tsubakino T, Hoshikawa T, Nakagawa T, Inawashiro T, Takahashi K, Suda M, Aizawa T. Imaging diagnosis of lumbar foraminal stenosis in the fifth lumbar nerve root: reliability and reproducibility of T1-weighted three-dimensional lumbar MRI. *J Spine Surg* 2021;7(4):502-509. doi: 10.21037/jss-21-63